SIAM J. NUMER. ANAL.
Vol. 22, No, 6, December 1985

A LARGE TIME STEP GENERALIZATION OF GODUNOV'S METHOD FOR SYSTEMS OF CONSERVATION LAWS*

RANDALL J. LEVEQUE†

Abstract. A generalization of Godunov's method for solving systems of conservation laws is proposed which can be applied for arbitrarily large time steps. Interactions of waves from neighboring Riemann problems are handled in an approximate but conservative manner that is exact for linear problems. For nonlinear systems it is found that better accuracy and sharper resolution of discontinuities is often obtained with Courant numbers somewhat larger than those allowed in Godunov's method. We explore the reasons for this behavior and, more generally, the effects of approximating wave interactions linearly. This linearization is easy to implement and may also be useful in other contexts, such as mesh refinement or shock tracking. A large time step generalization of the random choice method is also mentioned.

1. Introduction. We are concerned with computing numerical approximate solutions to systems of conservation laws of the form

$$u_t + f(u)_x = 0, \qquad -\infty < x < \infty, \quad t \geqq 0. \tag{1.1}$$

Here $u \in \mathbb{R}^m$, $f: \mathbb{R}^m \to \mathbb{R}^m$. We assume that the system is strictly hyperbolic, i.e. that the Jacobian matrix $\partial f/\partial u$ has distinct real eigenvalues for each value of u. Moreover we assume that each characteristic field is either genuinely nonlinear or linearly degenerate in the sense of Lax [15].

It is well known that solutions to (1.1) can develop discontinuities (e.g., shocks) even if the initial data is smooth. One then seeks a weak solution to (1.1), a function $u(x, t)$ which satisfies

$$\int_0^\infty \int_{-\infty}^\infty u(x,t)\varphi_t(x,t) + f(u(x,t))\varphi_x(x,t)\, dx\, dt + \int_{-\infty}^\infty u(x,0)\varphi(x,0)\, dx = 0$$

for all C_0^1 test functions $\varphi(x, t)$. We are primarily concerned with the computation of such discontinuous solutions and particularly with achieving high resolution of the discontinuities themselves.

Many numerical methods for solving such problems with general initial data are based on solutions to the more tractable Riemann problem, the equation (1.1) with special initial data consisting of two constant states separated by a single discontinuity

$$u(x,0) = \begin{cases} u_L, & x < \xi, \\ u_R, & x \geqq \xi. \end{cases} \tag{1.2}$$

For equations of the class considered here, this problem has a similarity solution of the form $u(x, t) = V(x-\xi)/t$ which consists of m waves. Each of these is either a shock or rarefaction wave (in a genuinely nonlinear field) or a contact discontinuity (in a linearly degenerate field) [15].

The classical numerical method based on solutions to Riemann problems is due to Godunov [8]. In this method the solution $u(x, t)$ at the time t_n is approximated by

* Received by the editors May 15, 1984. This work was supported in part by a National Science Foundation Postdoctoral Fellowship and by the Courant Institute of Mathematical Sciences, New York University, New York.

† Department of Mathematics, University of California at Los Angeles, Los Angeles, California 90024.

a piecewise constant function $u^n(x, t_n)$ taking the value U_i^n on the ith mesh cell $(x_i, x_{i+1}]$,

$$u^n(x, t_n) = U_i^n \quad \text{for } x_i < x \leqq x_{i+1}. \tag{1.3}$$

Here $x_j = jh$ and $t_n = nk$ where h and k are the mesh width and time step respectively. For $t > t_n$ the discontinuity at each x_i resolves into m waves. For $t - t_n$ sufficiently small the solution $u^n(x, t)$ is obtained by simply piecing together the solutions to the sequence of Riemann problems determined by the discontinuities. Eventually, waves arising from neighboring discontinuities begin to interact (in a complicated manner) and the solution $u^n(x, t)$ is no longer easy to determine. In Godunov's method one chooses a time step k sufficiently small that no interaction occurs and hence the exact solution $u^n(x, t_{n+1})$ at time $t_{n+1} = t_n + k$ can be computed. To prepare for the next time step this solution is replaced by a new piecewise constant approximation $u^{n+1}(x, t_{n+1})$ of the general form (1.3). The value U_i^{n+1} is obtained by averaging $u^n(x, t_{n+1})$ over $(x_i, x_{i+1}]$:

$$U_i^{n+1} = \frac{1}{h} \int_{x_i}^{x_{i+1}} u^n(x, t_{n+1})\, dx. \tag{1.4}$$

The *Courant number* ν corresponding to the mesh width h and time step k is defined as k/h times the maximum wave speed of waves arising in the solution $u^n(x, t)$. It is the maximum number of mesh cells (or fraction of a mesh cell) through which a wave can propagate in one time step.

It is clear that Godunov's method is applicable if the Courant number is less than $\frac{1}{2}$, for then waves travel at most halfway through a mesh cell and cannot interact with waves from neighboring discontinuities. In fact this restriction is easily relaxed to allow Courant numbers up to 1. Although the solution $u^n(x, t_{n+1})$ may then involve interactions and may not be easy to compute, the average (1.4) can still be determined by integrating the conservation law over the rectangle $[x_i, x_{i+1}] \times [t_n, t_{n+1}]$. In this manner one also obtains a formula for Godunov's method in conservation form. (cf. [20]).

For larger Courant numbers this is not the case and in general neither $u^n(x, t)$ nor even its average can be computed at time t_{n+1}. Here we explore the possibility of generalizing Godunov's method to larger time steps by using an approximate solution $\tilde{u}^n(x, t)$ which can be computed at time t_{n+1}. This approximate solution is then averaged as in (1.4) to give initial data for the next time step.

The approximate solution we use agrees with the true solution until interactions occur. The interactions are then handled approximately by allowing waves to simply pass through one another with no changes in speed or strength and with no creation of new waves. In this sense they behave as waves in the solution to a linear problem $u_t + Au_x = 0$ would.

Note that for weak waves (arising, for example, from the discretization of a smooth solution, where the discontinuities are $O(h)$), wave interactions are in fact nearly linear and so $\tilde{u}^n(x, t)$ may be a good approximation to $u^n(x, t)$ in this case.

In the standard Godunov method errors are introduced only by the averaging process (1.4). Now we are introducing errors into the solution $\tilde{u}^n(x, t)$. However, by taking larger time steps the averaging step is performed less frequently thereby reducing those errors. The numerical results of § 3 and a rough error analysis in § 5 both indicate that for smooth solutions the new errors introduced may be no worse than the averaging errors being eliminated. Consequently the algorithm is relatively insensitive to increases in the Courant number on smooth solutions.

Our main interest, however, is in resolving shocks and contact discontinuities

sharply and here it seems that a linear approximation of interactions is inappropriate. Surprisingly, it is found numerically that the large time step method with moderate values of the Courant number (larger than 1 but smaller than 3, say) often has much higher resolution than Godunov's method. Of course the smearing of shocks which is characteristic of Godunov's method is again caused by the averaging (1.4) and so an increase in the time step might be expected to decrease the rate of smearing. This would certainly be true if the interactions were handled correctly. In §§ 4 and 5 we attempt to explain why the difficulties caused by approximating these interactions are not as serious as one might expect.

In fact it seems that with larger time steps shocks are in some sense more compressive than in Godunov's method. In § 4 we show that for scalar problems any shock can be confined to a finite number of mesh points for all time if the Courant number is sufficiently large. If the Courant number is chosen properly there even exist one-point traveling shocks.

These positive results indicate that the large time step generalization of Godunov's method may be a useful method in its own right. In addition, it is possible that this approach to approximating wave interactions will find applications in generalizing other methods to larger time steps or in implementing Godunov-type methods in cases where it is convenient to let the Courant number stray above 1 occasionally. This is true on nonuniform grids where Godunov's method is easily applied but the timestep is traditionally restricted by the smallest mesh width. For example, Harten and Hyman [13] have devised a promising method in which each mesh point moves according to a weighted average of wave speeds arising from that discontinuity. They must ensure that the mesh points are always well separated in order to use a constant time step, but this may be unnecessary if the Courant number restriction is removed. Relaxation of this restriction could also prove useful in local mesh refinement.

Another possible application is to shock tracking where, in addition to a fixed mesh, additional points representing shocks are introduced and allowed to move independently. This avoids any smearing of strong discontinuities. Since the shocks may fall arbitrarily close to the fixed mesh points, it might again be useful to approximate interactions linearly.

For steady state calculations there is reason to believe that the large time step method would not give an adequate converged solution and indeed probably would not even reach a numerical steady state. However, this algorithm might be very useful in the early phases of such calculations. Traditional explicit algorithms suffer in steady-state calculations from the slow propagation speeds (measured in mesh cells per time step) imposed by Courant number restrictions. The large time step method avoids this drawback and may make it possible to obtain an approximate steady state solution very quickly, then switching to a different method to complete the calculation.

We do not pursue any of these applications here. The intent of this paper is to present the basic algorithm as a generalization of Godunov's method and to explore some of the effects of approximating interactions linearly.

This work was originally inspired by Roe's observation [26], [27] that finite difference schemes for conservation laws can profitably be viewed in terms of the propagation of information. A related method, at least for scalar conservation laws, is being studied by Brenier [1], [2]. In his Transport Collapse method a multivalued solution is obtained over large time steps and then collapsed into a single-valued approximation. The method described here can be improved for scalar problems by dispensing with the approximation and handling interactions exactly even over very large time steps [18].

2. The large time step generalized method. The large time step generalization of Godunov's method will be introduced more precisely in three different forms. (For a fourth version see Brenier [1].) First we define an approximate solution $\tilde{u}^n(x, t)$ for all $t \geqq t_n$ by combining solutions to the individual Riemann problems posed at time t_n. This approximate solution can then be averaged as in (1.4) to obtain U_i^{n+1}. Second, we rewrite the method as a conservation form scheme for the U_i^{n+1}. This form is useful for theoretical analysis [20]. Finally, we reformulate the method in the way it is actually implemented: each discontinuity is considered in turn and resolved into waves which are propagated independently over the mesh.

Let $u_j^n(x, t)$ denote the solution for $t \geqq t_n$ to the Riemann problem (1.1) with initial data consisting of a single discontinuity at x_j, i.e., with initial data

$$u_j^n(x, t_n) = \begin{cases} U_{j-1}^n, & x < x_j, \\ U_j^n, & x \geqq x_j. \end{cases} \tag{2.1}$$

Then the approximate solution $\tilde{u}^n(x, t)$ to (1.1) with initial data (1.3) is defined (for $t \geqq t_n$) by

$$\tilde{u}^n(x, t) = u^n(x, t_n) + \sum_j (u_j^n(x, t) - u_j^n(x, t_n)). \tag{2.2}$$

This is always a finite sum. If the Courant number is denoted by $\nu = k/h \times$(max. wave speed) then the summand is nonzero only for those values of j with $|x - x_j| < \nu h$.

For $t - t_n$ sufficiently small, $\tilde{u}^n(x, t)$ is equal to the exact solution $u^n(x, t)$. For larger t, $\tilde{u}^n(x, t)$ can be interpreted as an approximate solution obtained by allowing waves to pass through one another with no change in speed or strength and with no creation of new waves in the other characteristic families. This is precisely the way waves interact in a linear problem $u_t + Au_x = 0$ and in fact it is easy to verify that for a linear problem $\tilde{u}^n(x, t) \equiv u^n(x, t)$ for all $t \geqq t_n$.

We can also interpret (2.2) as shown in Fig. 2.1. The value of $\tilde{u}^n$ at a point (x, t) is equal to the initial value at (x, t_n) plus the jump in u across all waves that cross the line segment connecting (x, t_n) and (x, t).

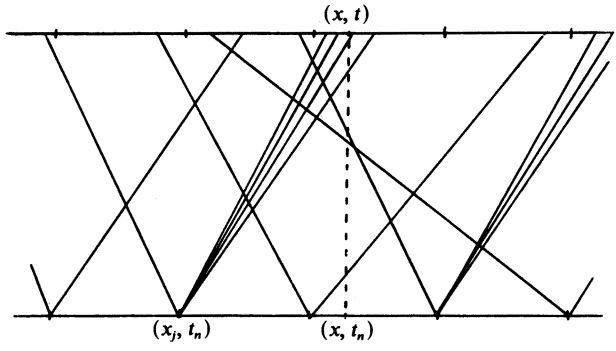

FIG. 2.1

The new piecewise constant approximation U_i^{n+1} at time t_{n+1} is obtained by averaging $\tilde{u}^n(x, t_{n+1})$ as in (1.4). This approximation is well defined for any size timestep.

Next we will rewrite the method in the conservation form

$$U_i^{n+1} = U_i^n - \frac{k}{h}[F(U^n; i+1) - F(U^n; i)] \tag{2.3}$$

with $F(U^n; i)$, the numerical flux function, a function of the values U_j^n for j near i. It is shown in [20] that this can be done by taking

$$F(U^n; i) = f(U_i^n) + \frac{1}{k}\sum_j \int_{t_n}^{t_{n+1}} [f(u_j^n(x_i, t)) - f(u_j^n(x_i, t_n))]\, dt. \tag{2.4}$$

Note that again this is always a finite sum and that the range of summation and hence the stencil of (2.3) automatically increase with ν so that the CFL condition is always satisfied.

The numerical flux F is consistent with the flux f in the sense that if $U_j^n \equiv U$ for all j with $|i-j| < \nu$ then

$$F(U^n; i) = f(U).$$

Moreover, F is Lipschitz continuous in each U_j^n. It follows by a theorem of Lax and Wendroff [16] that for any fixed mesh ratio k/h (arbitrarily large), if the numerical approximation converges to a limit $u(x, t)$ as the mesh is refined, then $u(x, t)$ is a weak solution to (1.1). In particular if the sequence of approximants has bounded total variation then by compactness there exists a convergent subsequence. Convergence of this method is discussed in more detail in [20].

DiPerna [6] has recently proved convergence of Godunov's method for a general class of systems of two equations using compensated compactness. This approach avoids the need for total variation bounds but has not been extended to the large time step generalization. Here we will assume total variation stability but, as we will see in § 3, this assumption may not be valid for large Courant numbers on nonlinear systems of equations.

In the special case of a scalar conservation law, the generalized method is stable. In fact, it is total variation diminishing (TVD) for all values of the Courant number and hence there is always a convergent sequence of approximants.

The two formulations of the generalized method presented so far both involve integrating the Riemann solutions $u_j^n(x, t)$, either in space (when applying (1.4) to (2.2)), or in time (when evaluating (2.4)). This is not a practical procedure, particularly when the Riemann solutions involve rarefaction waves. Instead the method is best implemented by "propagating waves" in a manner inspired by Fig. 2.1.

Consider a single wave emanating from the discontinuity at (x_j, t_n). Suppose it is either a shock or a contact discontinuity so that the wave consists of a jump discontinuity of strength $\Delta u = u_L - u_R$ propagating at some speed s. We will consider the effect that this wave has on the transformation from U^n to U^{n+1}.

If the wave propagates entirely through the interval $[x_i, x_{i+1}]$ then at each point $x \in [x_i, x_{i+1}]$ the approximate solution $\tilde{u}^n$ is incremented by Δu during $[t_n, t_{n+1}]$, so that the cell average is also incremented by Δu. If the wave propagates a fraction of the way through the interval (so that it is at some point ξ, $x_i < \xi < x_{i+1}$, at time t_{n+1}), then the cell average is incremented by the corresponding fraction of Δu:

$$\frac{\xi - x_i}{h}\Delta u \quad \text{if } s > 0 \quad \text{or} \quad \frac{\xi - x_{i+1}}{h}\Delta u \quad \text{if } s < 0.$$

This tells how to propagate a single wave and due to the linear interaction of waves in the approximate solution, each wave can be propagated independently of all other waves. This gives the following algorithm for computing U_i^{n+1}.

ALGORITHM 2.1
Initialize $U_i^{n+1} = U_i^n$ for all i.
For each j do
  resolve the discontinuity at x_j into m waves
  for each wave do
    set $\nu = sk/h$, $\mu = \lfloor \nu \rfloor$
    for $i = 0, 1, \cdots, \mu - 1$ do
      $U_{i+1}^{n+1} := U_{i+1}^{n+1} + \Delta u$
    $U_{i+\mu}^{n+1} := U_{i+\mu}^{n+1} + (\nu - \mu)\Delta u$

Here s is the wave speed and Δu the jump in u across the wave in question. We have assumed that $s \geqq 0$ for all waves so that propagation is always to the right. More generally, waves with speed $s < 0$ would be propagated to the left in an analogous manner.

This algorithm works fine provided all of the waves are discontinuities. Rarefaction waves introduce a new difficulty, particularly since with larger Courant numbers the rarefaction fan may span several mesh cells at time t_{n+1}. The approach taken here is to allow only sharp discontinuities which will be propagated as in Algorithm 2.1. There are various ways to approximate rarefaction fans. The optimal approach is to calculate a sequence of discontinuities and corresponding propagation speeds so that the jumps propagate exactly to mesh points and yield precisely the projection of the true rarefaction wave onto the mesh. This depends on our ability to explicitly integrate the rarefaction fan to obtain the averages (1.4). For the Euler equations this can be done efficiently and this technique has been used in the experiments of § 3.

Another possibility is to replace each rarefaction wave by a sequence of entropy-violating shocks which will spread out to approximate the true rarefaction wave as time evolves. By using sufficiently many shocks we obtain an approximation which, once projected back onto the grid by (1.4), is qualitatively indistinguishable from what would be obtained using the true rarefaction. This is the approach that was used in [18] for scalar problems and is used on the isentropic Euler equations example of § 3 (see [19] for details).

A final possibility is to use a piecewise linear approximation to the flux function in the original conservation law. Then each Riemann solution involves only discontinuities. This approach has been used by Dafermos [5] to obtain existence results and by Swartz and Wendroff [29] in numerical calculations with the Euler equations, where a piecewise linear equation of state is used.

3. Numerical results. Before analyzing the method in any detail it is useful to consider some numerical examples that illustrate the possibilities and limitations of this method. Numerous experiments have shown that linearizing the interactions is generally not detrimental at modest values of the Courant number. In fact, better accuracy and sharper resolution is often obtained with Courant numbers ν slightly larger than 1 than with the standard Godunov method.

We also present some results with much larger values of ν. Here the solution deteriorates considerably but some interesting phenomena are observed which lead to a better understanding of the effect of linearization. These experiments suggest certain theoretical results that help to justify the use of this linearization at more practical values of the Courant number.

We begin by considering a system of 2 conservation laws where it will be easier to explain the observed behavior in the phase plane. The system we use was suggested by Roe [26] as a model problem but it also arises in the study of gas flow in pipelines

(cf. [22]). It is obtained from the isentropic Euler equations by setting $\gamma = 1$:

$$\rho_t + m_x = 0, \qquad m_t + (m^2/\rho + a^2\rho)_x = 0. \tag{3.1}$$

Here ρ and m represent density and momentum respectively and a is the constant sound speed. Implementation details for the large time step method on this system are summarized in [19].

As a numerical example, the following initial conditions have been used:

$$u(x,0) = \begin{cases} u_1, & 0 \leqq x < 0.1, \\ u_2, & 0.1 \leqq x < 0.5, \\ u_4, & 0.5 \leqq x < 0.98, \\ u_5, & 0.98 \leqq x \leqq 1, \end{cases}$$

where

$$u_1 = \begin{bmatrix} 0.5 \\ 0.111803 \end{bmatrix}, \quad u_2 = \begin{bmatrix} 0.4 \\ 0 \end{bmatrix}, \quad u_4 = \begin{bmatrix} 0.2 \\ 0 \end{bmatrix}, \quad u_5 = \begin{bmatrix} 0.35 \\ -0.19843 \end{bmatrix}.$$

We take $a = 1$. The states u_1 and u_2 are separated by a shock moving to the right, u_4 and u_5 by a shock moving to the left. The states u_2 and u_4 are separated by a rarefaction moving to the left, an intermediate state

$$u_3 = \begin{bmatrix} 0.28260 \\ 0.098185 \end{bmatrix},$$

and a shock moving to the right. We compare computed and exact solutions at time 0.16, before any interaction has occurred, and at time 0.32, after the shock separating u_1 and u_2 has interacted with the rarefaction separating u_2 and u_3 and the two shocks in the right half of the interval have also interacted. Fig. 3.1 shows the true solution in the x-t plane.

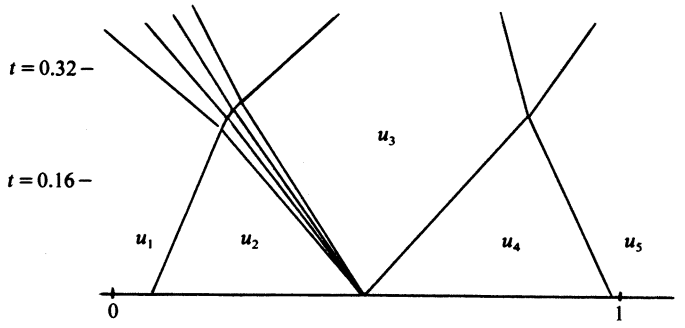

FIG. 3.1. *The structure of the true solution in the x-t plane for the first example.*

For this problem the Courant number is roughly $\nu \approx 1.5\lambda$, where $\lambda = k/h$. Figs. 3.2 and 3.3 show computations with $h = 1/50$ and various values of λ. For $\lambda = 0.5$, $\nu < 1$ and we have Godunov's method. Note the excessive smearing of shocks. Taking $\lambda = 1$ gives a dramatic improvement. Another slight improvement is seen going to $\lambda = 2$. For $\lambda = 4$ and 8 the results at $t = 0.16$ continue to improve but the interactions are handled poorly and the results at $t = 0.32$ are completely incorrect in some regions.

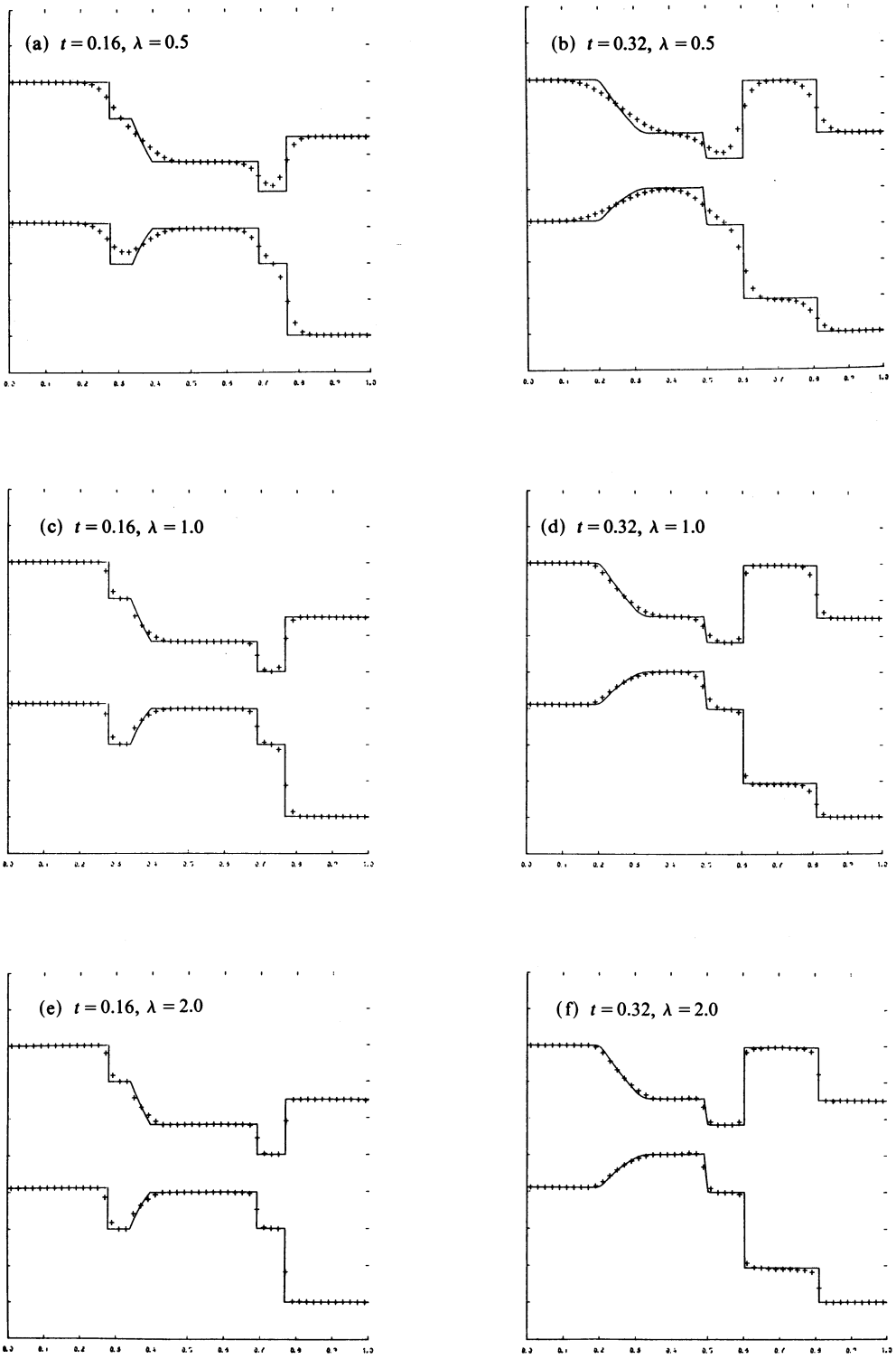

FIG. 3.2. *Solutions ρ (upper curve) and m (lower curve) obtained with $h = 1/50$ and various $\lambda = k/h$.*

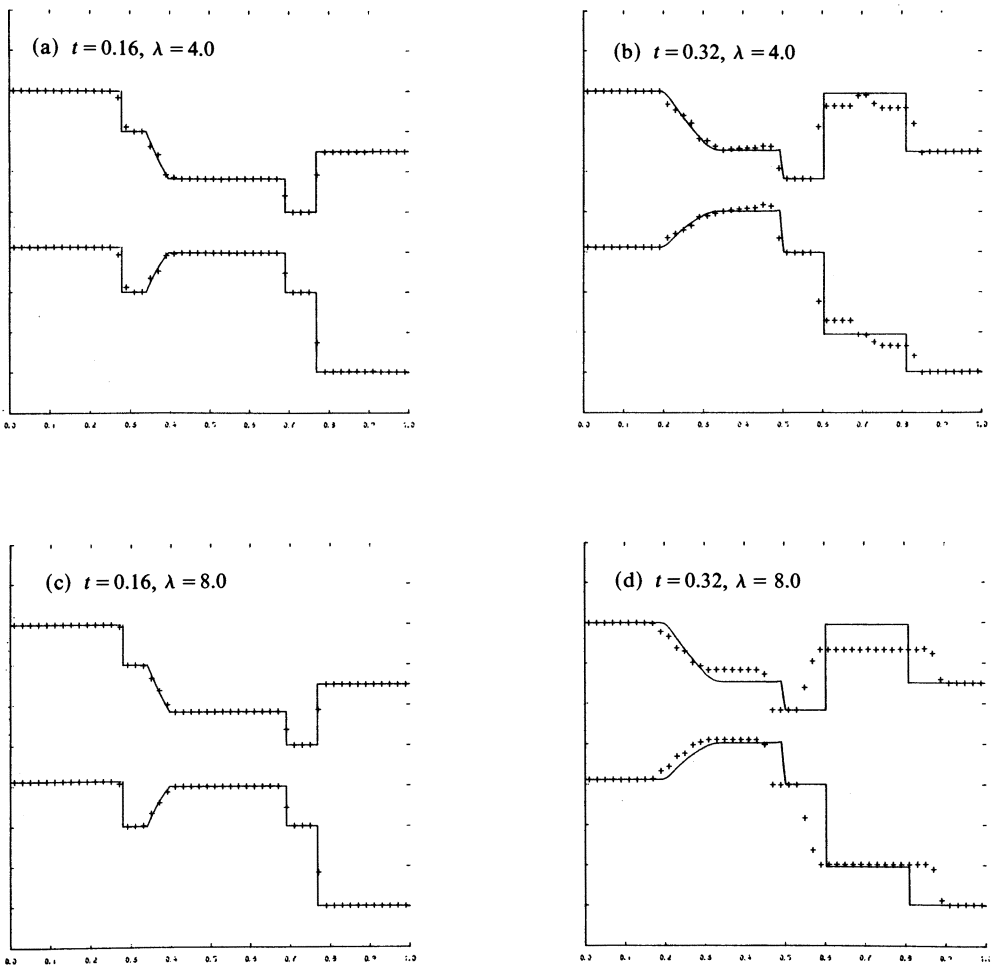

FIG. 3.3. *Solutions ρ (upper curve) and m (lower curve) obtained with $h=1/50$ and various $\lambda=k/h$.*

For $\lambda=4$ and 8 the same computations have been repeated with $h=1/100$ (Fig. 3.4). Note that with fixed mesh ratio the results have improved over Fig. 3.3. Also note that for $\lambda=8$, $h=1/100$ the results are very similar to the previous results with $\lambda=4$, $h=1/50$. In each case 2 time steps are taken between $t=0.16$ and $t=0.32$. In the first of these, the shock interaction is approximated linearly and an incorrect state is generated (the same state is visible in Fig. 3.4d where only a single time step has occurred since $t=0.16$). In the second step waves propagating back into the interaction zone from each discontinuity tend to correct the solution. This mechanism is explored in § 5.

Next we consider the full Euler equations,

$$\rho_t+(\rho u)_x=0,$$
$$(\rho u)_t+(\rho u^2+p)_x=0,$$
$$E_t+((E+p)u)_x=0,$$

where $E=p/(\gamma-1)+\frac{1}{2}\rho u^2$ and $\gamma=1.4$. Algorithms for solving the Riemann problem

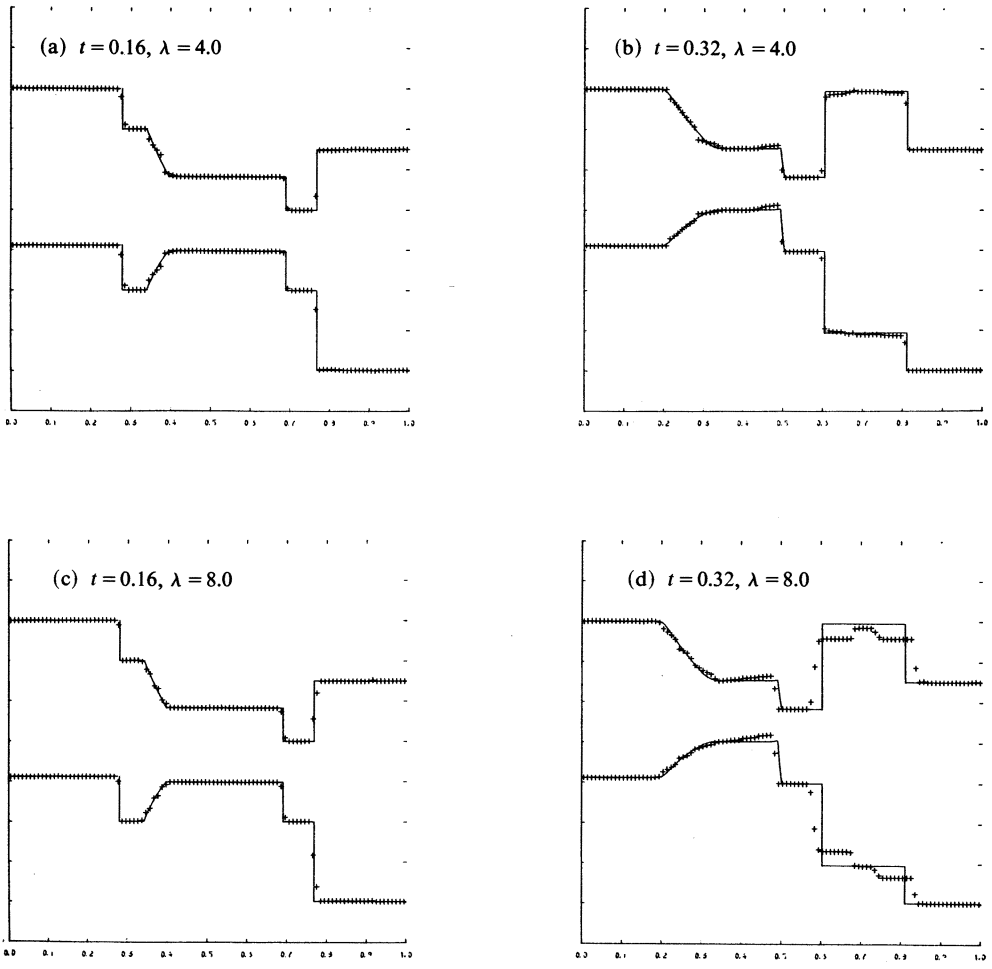

FIG. 3.4. *Solutions ρ (upper curve) and m (lower curve) obtained with $h = 1/100$ and various $\lambda = k/h$.*

for this system can be found in [3] or [28]. Rarefaction waves have been handled by computing the exact integral of each rarefaction fan over each mesh cell. Details and further experiments will be reported on elsewhere. Here we simply present a few results.

The first example gives another illustration of the "self-correction" phenomenon seen with the 2×2 system. The initial conditions are the following:

$$\text{for } x < 0.6: \quad \rho = 0.265574, \quad u = 0.927453, \quad p = 0.303130;$$

$$\text{for } 0.6 \leqq x \leqq 0.65: \quad \rho = 0.125, \quad u = 0, \quad p = 0.1;$$

$$\text{for } 0.65 < x: \quad \rho = 0.516633, \quad u = -2.66908, \quad p = 1.27472.$$

The two discontinuities are shocks which collide at time $t = 0.0095$ and produce two outgoing shocks with a contact discontinuity in between. Applying the method with $\lambda = 1$ (which corresponds to a Courant number $\nu \approx 3.5$) gives the results shown in Fig. 3.5. Here we are looking at a fixed grid and showing the density ρ after each time step. After a single time step (Fig. 3.5a) the shock interaction has been approximated linearly so that the numerical solution consists simply of two discontinuities (with some smearing). In later time steps (Fig. 3.5b, c, d) the true structure of the solution

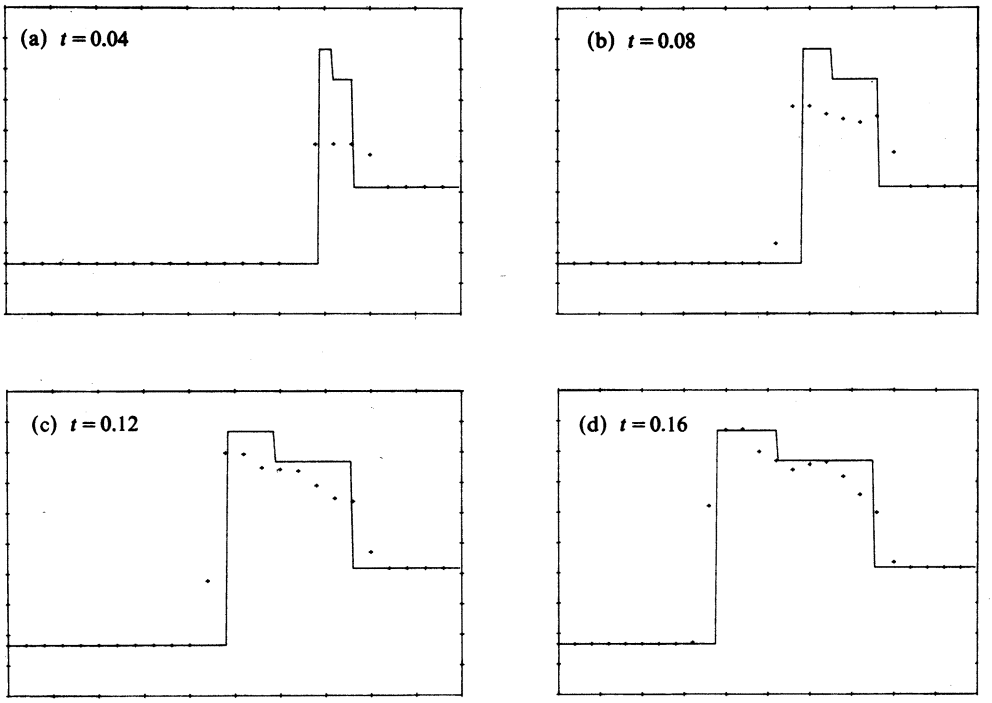

FIG. 3.5. *The density ρ computed with $k = h = 1/25$ and the true solution. (Courant number ≈ 3.5.)*

begins to reemerge. There are two interesting questions. First, does the solution on this fixed grid have the correct long time behavior in some sense as $t \to \infty$? Of course we expect smearing of the discontinuities that will not disappear as $t \to \infty$, but do we have convergence to the true solution away from the discontinuities? The second question is whether we have convergence at a fixed time as the mesh is refined. Actually these two questions are virtually identical. Due to the fact that the solution to each Riemann problem is a similarity solution invariant under an identical rescaling of x and t, a solution obtained at a fixed time with a finer grid is simply a rescaling of the solution which would be obtained at a larger time on the original grid. (Actually, for this to be strictly true one needs to also rescale the initial conditions as is done in § 5. However, for the simple example we are considering this makes little difference in the structure of the solution.) Thus, Fig. 3.6, which shows the solutions at $t = 0.08$ and

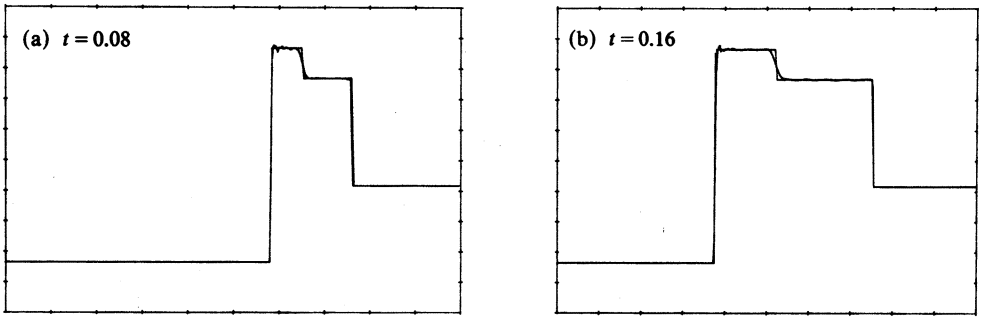

FIG. 3.6. *The density ρ computed with $k = h = 1/400$ superimposed on the true solution. (Courant number ≈ 3.5.)*

0.16 obtained with $h = 1/400$ (and $\lambda = 1$) can equivalently be viewed as showing the solutions at $t = 12.8$ and 25.6 on the original grid with $h = 1/25$ (with the x-axis also rescaled by a factor of 16).

We see some oscillation near the leftmost shock which do not die away as $t \to \infty$. On the other hand they also do not grow in amplitude and seem to be localized near the shock. With smaller values of the Courant number these oscillations are reduced in magnitude and convergence looks quite good.

With larger Courant numbers the situation can look quite bad. Fig. 3.7 again shows $t = 0.08$ and 0.16 with $h = 1/400$ but now with $\lambda = 2$ ($\nu \approx 7$). Here the oscillations are not confined near the shocks and do not diminish as $t \to \infty$. On the other hand, since Fig. 3.7b can also be viewed as the solution at $t = 0.08$ with $h = 1/800$ (by compressing the x-axis), it seems that the oscillations do have a higher frequency as the mesh is refined. We seem to have a situation in which the numerical solution converges weakly star in L_∞ but does not converge pointwise or in L_1. More will be said about this in § 5.

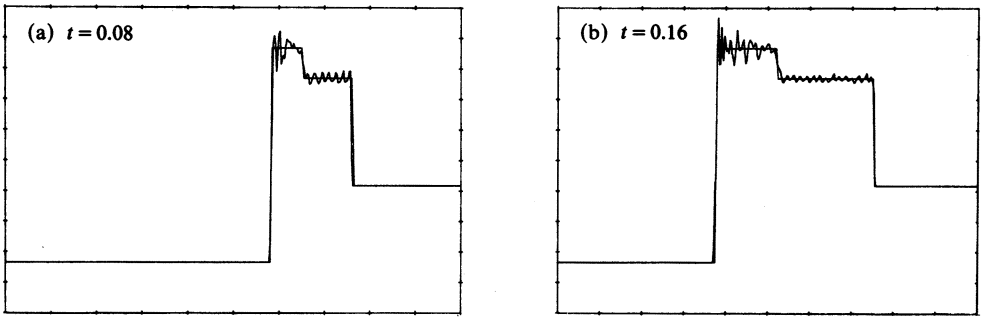

FIG. 3.7. *The density ρ computed with $h = 1/400$, $k = 2h$, superimposed on the true solution. (Courant number ≈ 7.)*

Finally, we consider an example with a smooth solution to show that in this case errors are relatively insensitive to increases in the Courant number. We used the initial data

$$\rho(x, 0) = 1 + 0.1 \sin(2\pi x),$$
$$(\rho u)(x, 0) = 0.1 \sin(4\pi x),$$
$$E(x, 0) = 0.5 + 0.1 \cos(2\pi x)$$

and periodic boundary conditions. Table 3.1 shows the errors in each component at $t = 0.32$. The max norm is used and the errors in each case were estimated by comparing to the solution obtained with 400 meshpoints and $\lambda = 1$. Here $\nu \approx 0.6\lambda$. We see that the method is first order accurate for each value of λ. Moreover, for a fixed mesh the errors are nearly as small with large time steps as with Godunov's method. The errors incurred by approximating interactions linearly are small for smooth solutions and apparently are no larger than those introduced by frequent averaging with smaller time steps. This is made more quantitative in § 5.

Fig. 3.8 shows the density solutions obtained at $t = 0.32$ with 400 points and $\lambda = 1$ (solid line) and with 50 points and $\lambda = 16$ (crosses). The latter solution (with $\nu \approx 9.6$) was obtained in a single timestep from the initial conditions which are also shown in Fig. 3.8 as a dashed line.

TABLE 3.1

Errors in the computed solutions ρ, ρu, and E at time $t = 0.32$ for a smooth solution. Errors were computed in the max norm by comparing with the solution obtained by using $n = 400$, $\lambda = 1$. ($h = 1/n$, $k = \lambda h$, and the Courant number $\nu \approx .6\lambda$)

λ	n	error in ρ	error in ρu	error in E
1	25	0.583 (−1)	0.225 (−1)	0.323 (−1)
	50	0.286 (−1)	0.118 (−1)	0.160 (−1)
	100	0.126 (−1)	0.552 (−2)	0.716 (−2)
2	25	0.135 (−1)	0.658 (−2)	0.751 (−2)
	50	0.677 (−2)	0.510 (−1)	0.563 (−2)
	100	0.452 (−2)	0.325 (−2)	0.304 (−2)
4	25	0.947 (−2)	0.399 (−2)	0.684 (−2)
	50	0.622 (−2)	0.362 (−2)	0.498 (−2)
	100	0.478 (−2)	0.266 (−2)	0.255 (−2)
8	25	0.230 (−1)	0.146 (−1)	0.252 (−1)
	50	0.118 (−1)	0.428 (−2)	0.803 (−2)
	100	0.588 (−2)	0.210 (−2)	0.324 (−2)
16	50	0.315 (−1)	0.115 (−1)	0.287 (−1)
	100	0.127 (−1)	0.389 (−2)	0.100 (−1)
32	100	0.306 (−1)	0.117 (−1)	0.305 (−1)

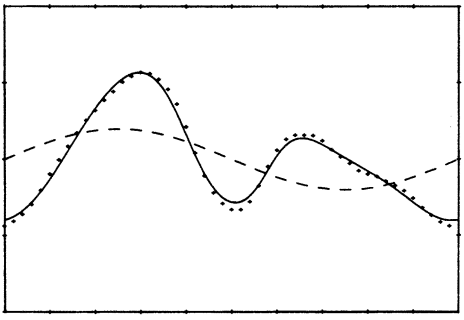

FIG. 3.8. *The density ρ at time $t = 0.32$ in a smooth solution, computed with $h = 1/50$ and $k = 16h = 0.32$. The solid line is the "true" solution, computed with $k = h = 1/400$. The dashed line shows the initial conditions.*

4. Analysis of the method for scalar problems. In this section we consider the behavior of the generalized method when applied to a scalar conservation law. This case is relatively easy to analyze and gives some justification for the experimental results of the previous section which show sharper shocks with Courant number larger than 1.

The extent to which this analysis carries over to systems of equations is discussed in the next section.

Consider the scalar problem

$$u_t + f(u)_x = 0 \tag{4.1}$$

with a convex flux function, $f''(u) > 0$, and nonincreasing data U^n which represents a

single shock smeared over a finite number of mesh points, e.g.,

$$
\begin{aligned}
&U_i^n = u_L && \text{for } i \leqq 0, \\
&U_i^n \leqq U_{i-1}^n && \text{for } 1 \leqq i \leqq M, \\
&U_i^n = u_R && \text{for } i \geqq M,
\end{aligned} \tag{4.2}
$$

with strict inequality at $i = 1$ and $i = M$. We say the shock is represented by M adjacent discontinuities and is confined to $M-1$ mesh cells (x_i, x_{i+1}), $i = 1, 2, \cdots, M-1$. To begin with suppose we are modelling a shock moving to the right and that $f'(u) > 0$ for $u_R \geqq u \geqq u_L$ so that all the discontinuities travel to the right.

The Courant number for this problem is

$$\nu = \lambda \max_{u_R \leqq u \leqq u_L} |f'(u)|.$$

If we apply Godunov's method with $\nu < 1$ then the discontinuity $U_1^n - U_0^n$ at x_1 travels a distance less than h in time k so that after averaging there will still be a discontinuity at x_1. The rightmost discontinuity at x_M will propagate at least partway into the interval (x_M, x_{M+1}) so that after averaging there will be a new discontinuity at x_{M+1}. As a result, at time t_{n+1} there will be $M+1$ discontinuities and the shock will have spread to M mesh cells. As $n \to \infty$ the shock seems to spread without bound. Actually, there exists a steady state profile in which, although there are infinitely many discontinuities, the strength of the discontinuities decreases quickly away from the correct shock location [14], [24]. Nonetheless, there is, in some sense, an infinite smearing of the shock as shown schematically in Fig. 4.1a.

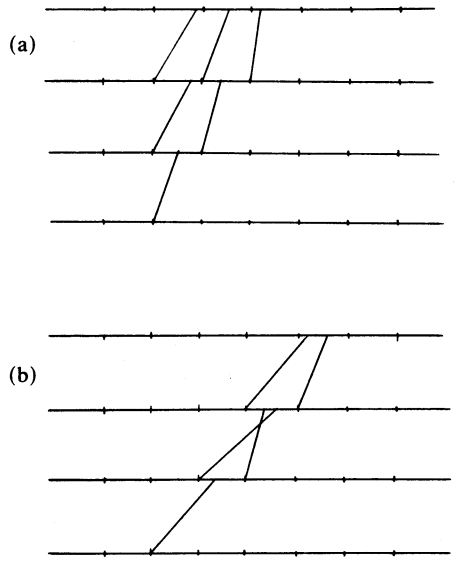

FIG. 4.1

With Courant numbers larger than 1, on the other hand, it is possible to confine a shock to a finite number of mesh points for all time. As a trivial example consider Burgers' equation $u_t + uu_x = 0$ with

$$U_i^0 = \begin{cases} 1 & \text{for } i \leqq 0, \\ 0 & \text{for } i > 0, \end{cases}$$

and $k=2h$. The discontinuity travels with speed $\frac{1}{2}$, moves exactly one mesh cell per time step, and is never smeared. The shock is represented numerically by a single discontinuity for all time.

Of course this is an unlikely situation, but the surprising and useful fact is that for any larger value of the mesh ratio, $k/h>2$, the shock is confined to a finite number of gridpoints for all time, the number being bounded by k/h. A typical case is shown in Fig. 4.1b. More generally we have

THEOREM 4.1. *Suppose that f is convex, $u_L>u_R$, and the mesh ratio $\lambda=k/h$ is chosen so that*

$$\lambda \min_{u_R\leqq u\leqq u_L} f''(u)\geqq \frac{2}{u_L-u_R}. \tag{4.3}$$

Then the shock can be confined to at most $N-1$ mesh cells for all time, where

$$N=\left|\lceil \lambda f'(u_L)\rceil - \lfloor \lambda f'(u_R)\rfloor\right|. \tag{4.4}$$

Here $\lceil x\rceil=\min\{n\in\mathbb{Z}: x\leqq n\}$ and $\lfloor x\rfloor=\max\{n\in\mathbb{Z}: x\geqq n\}$. Note that we have dropped the assumption $f'>0$ but if this holds then $N<\lceil \nu\rceil$ and for ν large enough that (4.3) is satisfied, the shock is confined to $\lceil \nu\rceil$ cells.

Proof. Suppose the shock is confined to $N-1$ mesh cells at time t_n with discontinuities only at $x_J, x_{J+1}, \cdots, x_{J+N}$ for some J. Let s_j be the speed of propagation of the shock initially at x_j,

$$s_j=\frac{f(U_j^n)-f(U_{j-1}^n)}{U_j^n-U_{j-1}^n}, \qquad j=J,\cdots,J+N.$$

Then the approximate solution $\tilde{u}^n(x,t_{n+1})$ is piecewise constant with discontinuities at the points

$$z_j=x_j+ks_j, \qquad j=J,\cdots,J+N.$$

Note that $f'(u_R)\leqq s_j\leqq f'(u_L)$ for all j. We wish to show that the points z_j lie within $N-1$ contiguous mesh cells so that averaging $\tilde{u}^n(x,t_{n+1})$ yields a mesh function U^{n+1} which again has at most N discontinuities.

Let

$$\underline{z}=\min\{z_j\}, \qquad \bar{z}=\max\{z_j\}$$

and let $\underline{x}$, $\bar{x}$ be the preimages of these points, e.g. $\underline{x}=x_j$ with j minimizing z_j. Denote the respective shock speeds by $\underline{s}$ and $\bar{s}$. It suffices to show that $\underline{z}$ and $\bar{z}$ lie within $N-1$ contiguous cells. We must consider three cases.

Case 1. $\underline{x}>\bar{x}$ and $\underline{s}\bar{s}\geqq 0$. In this case the extremal shocks originating at $\underline{x}$ and $\bar{x}$ cross in time t (since $\bar{z}>\underline{z}$) and are both moving in the same direction. Without loss of generality, suppose they are both moving to the right. We have $\underline{s}\geqq f'(u_R)$ so the shock at $\underline{x}$ propagates entirely through at least $\lfloor \lambda f'(u_R)\rfloor$ cells. Since $\bar{s}\leqq f'(u_L)$ the discontinuity at $\bar{x}$ propagates through at most $\lceil \lambda f'(u_L)\rceil$ cells. Since $\underline{x}$ and $\bar{x}$ are at least one cell apart, it follows that $\underline{z}$ and $\bar{z}$ lie within

$$\left|\lceil \lambda f'(u_L)\rceil - \lfloor \lambda f'(u_R)\rfloor\right| - 1 = N-1$$

contiguous cells.

Case 2. $\underline{x}>\bar{x}$ and $\underline{s}\bar{s}<0$. In this case the shocks are traveling in opposite directions and cross. The shock from $\bar{x}$ is traveling to the right and propagates through at most $\lceil \lambda f'(u_L)\rceil$ cells. The shock from $\underline{x}$ is traveling to the left and propagates through at

most $-\lfloor \lambda f'(u_R) \rfloor$ cells. Since the shocks cross, these two sets overlap by at least one cell and so $\underline{z}$ and $\bar{z}$ lie within at most

$$\lceil \lambda f'(u_L) \rceil + (-\lfloor \lambda f'(u_R) \rfloor) - 1 = N - 1$$

contiguous cells.

Case 3. $\underline{x} < \bar{x}$. In this case the extremal shocks do not cross and we will show that $\bar{z} - \underline{z} \leqq (N-2)h$ so that they necessarily lie within $N-1$ contiguous cells. Since $\underline{s} > \bar{s}$ we immediately have

$$\bar{z} - \underline{z} \leqq \bar{x} - \underline{x} \leqq (N-1)h.$$

Moreover $\bar{z} - \underline{z} \leqq (N-2)h$ unless $\bar{x} - \underline{x} = (N-1)h$, i.e., unless $\underline{x} = x_J$ and $\bar{x} = x_{J+N}$ so consider only this case. Then the discontinuity at $\underline{x}$ has u_L as its left state and the discontinuity at $\bar{x}$ has u_R as its right state. Since $\bar{z} - \underline{z} = (\bar{x} - \underline{x}) + k(\bar{s} - \underline{s})$ it suffices to show that $k(\bar{s} - \underline{s}) \leqq -h$. By convexity of f, $\bar{s} - \underline{s}$ is maximized by taking a single state u_1, say, between u_L and u_R so that

$$\underline{s} = \frac{f(u_L) - f(u_1)}{u_L - u_1}, \qquad \bar{s} = \frac{f(u_R) - f(u_1)}{u_R = u_1}.$$

Then

$$\underline{s} = f'(u_1) + \tfrac{1}{2}(u_L - u_1) f''(\underline{\nu}),$$
$$\bar{s} = f'(u_1) + \tfrac{1}{2}(u_R - u_1) f''(\bar{\nu}),$$

with $\underline{\nu}, \bar{\nu} \in [u_R, u_L]$. Hence

$$\underline{s} - \bar{s} = \tfrac{1}{2}(u_L - u_1) f''(\underline{\nu}) + \tfrac{1}{2}(u_1 - u_R) f''(\bar{\nu})$$
$$\geqq \tfrac{1}{2}(u_L - u_R) \min_{u_R \leqq \nu \leqq u_L} f''(\nu) \geqq \frac{h}{k}$$

by the condition (4.3). So $k(\bar{s} - \underline{s}) \leqq -h$ and the proof is complete.

Theorem 4.1 says that a shock confined to $N-1$ cells initially will remain confined to $N-1$ cells. One might wonder whether a shock initially spread over more than $N-1$ cells will eventually be compressed to $N-1$ cells. In general the condition (2.3) does not guarantee this but if we strengthen it slightly we have

THEOREM 4.2. *Suppose*

$$\lambda \min_{u_R \leqq u \leqq u_L} f''(u) \geqq \frac{4}{u_L - u_R}. \tag{4.5}$$

Then a shock initially confined to $M-1$ cells with $M \geqq N$ will be confined to at most $N-1$ cells (with N given by (4.4)) *within at most $M - N$ time steps.*

The proof is similar to the proof of Theorem 4.1 and will be omitted.

These theorems give an indication of why the large time step method performs better on shocks than might be expected, at least on a scalar problem. For systems the same sort of behavior is observed for an isolated shock of one family. In addition, for systems we must analyze the interaction of shocks from different families. This will be discussed in § 5.

We now turn our attention to the behavior of the algorithm on smooth solutions. For scalar problems this is easy to analyze although the analysis, unfortunately, does not carry over to systems. The solution is smooth in a given time step if no shocks form. This implies that characteristics do not cross and hence the discontinuities do not interact. Consequently, the approximate solution $\tilde{u}^n(x, t)$ is in fact the true solution

$u^n(x, t)$ (for the given piecewise constant initial data U^n). In this case errors are caused only by averaging at the end of a time step, which introduces $O(h^2)$ errors. This suggests that in order to compute a smooth solution up to some time T, it is optimal to use a single time step, $k = T$. Then the global error at time T will be $O(h^2)$. This gives second order accuracy as opposed to the traditional Godunov's method in which the global error is $O(h^2/k)$ and hence first order accurate since k/h is fixed as $h \to 0$. Note that fixing $k = T$ corresponds to the Courant number $\nu \to \infty$ as $h \to 0$.

To obtain this accuracy we must be careful to handle rarefaction waves properly. If these waves are approximated by entropy violating shocks then $\tilde{u}^n(x, t)$ is not the correct entropy solution. We must split the discontinuities into sufficiently many pieces that the spreading approximates the true spreading to second order.

For systems of equations there are interactions between waves of different families which occur even for smooth solutions and we cannot in general obtain second order accuracy. Note however that for a *linear* system the interactions are handled correctly, $\tilde{u}^n(x, t) \equiv u^n(x, t)$, and this analysis applies to show that here again it is optimal to take a single large time step.

Observe also that for linear systems of equations and for scalar conservation laws with smooth solutions, the large time step method is equivalent to the method of characteristics. The averaging process (1.4) used to project onto the grid at time t_{n+1} corresponds to the use of linear interpolation between the U_j^n in the method of characteristics.

5. Analysis on nonlinear systems of equations. On nonlinear systems of equations the analysis becomes much more difficult. Here we will only indicate why some of the counterintuitive numerical results of § 3 are in fact reasonable.

We first continue with the analysis of § 4 for smooth solutions. For systems of equations errors arise due to interactions between waves of different families. However, in a smooth solution the discontinuities introduced by discretizing are weak and so the interactions behave nearly linearly. Consequently, $\tilde{u}^n(x, t)$ should still be a good approximation to $u^n(x, t)$. More precisely, the discontinuities are $O(h)$ as $h \to 0$ and it can be shown that the error made in approximating an interaction linearly is $O(h^2)$. The error in $\tilde{u}^n(x, t_{n+1})$ will depend on the number of interactions which have occurred between t_n and t_{n+1}. This number is proportional to the Courant number ν and so we expect a cumulative error in $\tilde{u}^n(x, t_{n+1})$ that is $O(\nu h^2) = O(kh)$. In addition there is still the $O(h^2)$ error introduced by averaging so that we expect the total error over one time step to be $O(kh + h^2)$ and hence the global error at a fixed time to be $O(h + h^2/k)$. This indicates that for systems the method is at best first order accurate. We can no longer obtain second order accuracy by fixing k as $h \to 0$. But at least it seems that the error does not increase if we increase the time step. This conclusion is supported by the results of Table 3.1. We stress, however, that a more rigorous error analysis is needed.

Next considering shocks, we note that an isolated shock can no longer be confined to a finite number of grid points due to the fact that the averaging process introduces discontinuities which now give rise to waves in the other families. However, these waves should be relatively weak and have little effect on the dynamics of the shock. We can still expect that using Courant numbers somewhat larger than 1 will give sharper shocks than Godunov's method. This is clearly the case in the plots for $t = 0.16$ in Fig. 3.2.

A more interesting case to consider is the interaction of two shocks in different families, for here the error caused by approximating interactions linearly is most clearly

seen. Consider Fig. 3.3 for example. A single time step is taken between Fig. 3.3c and Fig. 3.3d. It is clear that the shock interaction in the right half of the interval has been handled incorrectly. The value of ρ in particular is far from correct (the upper graph in Fig. 3.3d) and the shocks are in the wrong positions. Fig. 5.1a shows the situation in the x–t plane, indicating why the shocks are in the wrong locations, and Fig. 5.1b shows the location of the states in the ρ–m plane (the phase plane). In these figures u_M^* represents the correct intermediate state after the collision and is connected to the states u_L and u_R by Hugoniot curves (see [19]). When the interaction is approximated linearly we instead obtain $\tilde{u}_M = u_L + u_R - u_M$. (Note that for a linear problem the characteristic curves for a given family would be parallel straight lines so that $\tilde{u}_M = u_M^*$.)

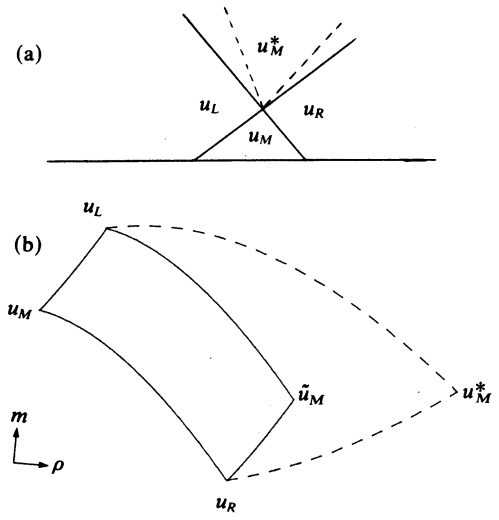

FIG. 5.1. (a) *shows the collision of two shocks in the x–t plane. The dashed line is the true resolution into outgoing shocks while the solid line is the linear approximation.* (b) *shows the true intermediate state* u_M^* *and the linear approximation* $\tilde{u}_M$ *in the p-m plane.*

Now consider the next time step. For clarity we ignore smearing of the discontinuities due to averaging and suppose that we start with the two sharp discontinuities from u_L to $\tilde{u}_M$ and from $\tilde{u}_M$ to u_R. Solving the Riemann problems, these each resolve into two waves as indicated in Fig. 5.2a. The new states $\tilde{u}_{LM}$ and $\tilde{u}_{MR}$ lie on the Hugoniot curves of u_L and u_R respectively as shown in Fig. 5.2b. When the two approaching waves collide a new state $\tilde{\tilde{u}}_M = \tilde{u}_{LM} + \tilde{u}_{MR} - \tilde{u}_M$ is obtained. This state is shown in Fig. 5.2b and is apparently much closer to the true intermediate state u_M^*.

Looking at Fig. 3.3b we can see these secondary states $\tilde{u}_{LM}$, $\tilde{u}_{MR}$ and $\tilde{\tilde{u}}_M$. Here two time steps have been taken since Fig. 3.3a. After the first, the same intermediate state $\tilde{u}_M$ was obtained as in Fig. 3.3d. We see that $\tilde{\tilde{u}}_M$, appearing in the middle of the interval between the shocks, is indeed much closer to the true solution.

This sort of phase plane analysis provides some understanding of the phenomena seen in the numerical experiments. However, it appears hard to prove anything about the behavior as $t \to \infty$ using this approach, particularly for systems of more than 2 conservation laws. Instead, we will use the fact, mentioned earlier, that letting $t \to \infty$ on a fixed mesh is analogous to looking at a fixed time and refining the mesh.

We would like to show that, in some sense, the numerical approximation approaches the true solution as $t \to \infty$. We will assume that the initial conditions are

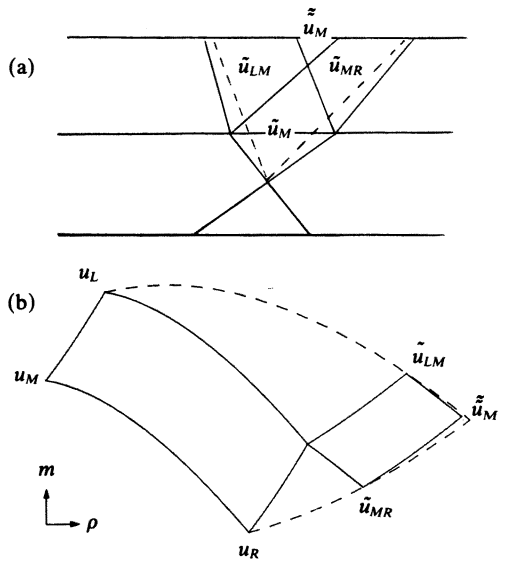

FIG. 5.2. *A second time step.* (a) *shows the new waves arising in the x–t plane.* (b) *shows the resulting states in the phase plane.*

of the form

$$u(x,0)=\begin{cases} u_L, & x<-N, \\ u_0(x), & -N\leqq x\leqq N, \\ u_R, & x>N, \end{cases} \tag{5.1}$$

where $u_0(x)$ has bounded variation. Liu [21] has considered the large-time behavior of the true solution for this problem and has shown that, as $t\to\infty$, $u(x,t)$ approaches $u^*(x,t)$ (at least away from discontinuities) where $u^*(x,t)$ is the solution to the Riemann problem with initial data

$$u^*(x,0)=\begin{cases} u_L, & x<0, \\ u_R, & x>0. \end{cases} \tag{5.2}$$

In particular, Liu shows that if the characteristic speeds $\lambda_j(u(x,t))$ are strictly separated, i.e., if there exist μ_i, $i=0,1,\cdots,m$ and $\delta>0$ such that $\lambda_i(u(x,t))-\delta<\mu_i<\lambda_{i+1}(u(x,t))+\delta$ for all x, t, then $u(x,t)\to u^*(x,t)$ as $t\to\infty$ for $x/t=\mu_i$ This is the type of result we would like to obtain for the numerical solution.

We must first assume that the total variation of the numerical approximation remains bounded as $t\to\infty$. This would seem to be a poor assumption in view of some of the numerical results of § 3 (e.g. Fig. 3.7). However, for smaller Courant numbers it does seem that the variation remains bounded. Moreover, the result presented here increases our confidence in the use of this linearization since it says that (at least in stable cases) the type of self-correcting behavior seen in Fig. 3.3 must be more general. Of course it would be very useful to obtain results on when the method is total variation stable. It would also be interesting to try to prove convergence in a weaker sense (say weak star in L_∞) in unstable cases.

Even assuming bounded variation we have not been able to prove pointwise convergence as for the exact solution but only the convergence to zero of an average error. However, as we note below, this gives pointwise convergence at "most" mesh points.

If U_i^n represents the numerical solution, then we let $U(x, t)$ be the piecewise constant function taking the value U_i^n on the (i, n) mesh cell. We have the following result, which holds not only for this generalization of Godunov's method but for any conservative method with consistent numerical flux.

THEOREM 5.1. *Consider* (1.1) *with the initial data of the form* (5.1) *and let* $U(x, t)$ *be the numerical solution generated by any scheme in conservation form. Suppose that the total variation of* $U(\cdot, t)$ *is bounded for all* t. *Then for any real numbers* $\delta > 0$, $m_1 < m_2$,

$$\frac{1}{t^2}\int_t^{t(1+\delta)}\int_{tm_1}^{tm_2} |U(x,\tau) - U^*(x,\tau)|\, dx\, d\tau \to 0 \tag{5.3}$$

as $t \to \infty$, *where* $U^*(x, \tau)$ *is some weak solution to the Riemann problem with data* (5.2).

Although this result is not as strong as one might hope for, note that it does guarantee that in any wedge $m_1 < x/t < m_2$ we eventually find values arbitrarily close to the true solution. In fact, since the rectangle $[t, t(1+\delta)] \times [tm_1, tm_2]$ contains $O(t^2)$ mesh points as $t \to \infty$, we can conclude from (5.3) that for any $\varepsilon > 0$, by taking t sufficiently large we have $|U(x, t) - U^*(x, t)| > \varepsilon$ for at most εt^2 of those mesh points. In this sense we have pointwise convergence at "most" of the mesh points.

Proof. Let the method be written in conservation form as

$$U_i^{n+1} = U_i^n - \frac{k}{h}[F_{i+1}^n - F_i^n], \tag{5.4}$$

with a slight change in notation from (2.3). Now set

$$U_j(x, t) = U(jx, jt), \qquad j = 1, 2, \cdots. \tag{5.5}$$

Then $U_j(x, t)$ is a piecewise constant function on a finer grid (with $\Delta x = h/j$ and $\Delta t = k/j$) and is in fact precisely the numerical approximation which would be obtained by applying (5.4) on this grid with the scaled initial data

$$u_j(x, 0) = u(jx, 0). \tag{5.6}$$

So we can view $U_j(x, t)$ as the numerical approximation to $u_j(x, t)$, the true solution with data (5.6).

Since the total variation of $U(\cdot, t)$ is bounded as $t \to \infty$ it follows by a standard compactness argument [7] that a subsequence of $\{U_j(x, t)\}$ converges as $j \to \infty$ to some function $U^*(x, t)$. We consider only this subsequence. We can show that $U^*(x, t)$ is a weak solution to the Riemann problem with data (5.2) in just the same way that Lax and Wendroff [16] originally showed convergence of schemes in conservation form. The only difference is that here the initial data $u_j(x, 0)$ changes as the mesh is refined (i.e., as $j \to \infty$). Let $U_{ji}^n = U_i^n$ but now viewed as an approximation to $u_j(ih_j, nk_j)$ where $h_j = h/j$, $k_j = k/j$. Choose a test function $\varphi \in C_0^1$ and set $\Phi_{ji}^n = \varphi(ih_j, nk_j)$. Multiplying (5.4) by Φ_{ji}^n, summing over n and i and performing summation by parts gives

$$0 = h_j k_j \sum_{n=0}^{\infty}\sum_{i=-\infty}^{\infty}\left\{U_{ji}^{n+1}\left(\frac{\Phi_{ji}^{n+1} - \Phi_{ji}^n}{k_j}\right) + F_{ji}^n\left(\frac{\Phi_{j,i+1}^n + \Phi_{ji}^n}{h_j}\right)\right\} + h_j \sum_{i=-\infty}^{\infty} \Phi_{ji}^0 U_{ji}^0.$$

As $j \to \infty$, this converges to

$$0 = \int_0^{\infty}\int_{-\infty}^{\infty} [U^*(x,t)\varphi_t(x,t) + f(U^*(x,t))\varphi_x(x,t)]\, dx\, dt + \int_{-\infty}^{\infty} \varphi(x,0)u^*(x,0)$$

which shows that $U^*(x, t)$ is a weak solution with initial data (5.2).

Since $U_j(x, t) \to U^*(x, t)$ it follows that for the given values of δ, m_1, and m_2,

$$\int_1^{1+\delta} \int_{m_1}^{m_2} |U_j(x, t) - U^*(x, t)| \, dx \, dt \to 0 \tag{5.7}$$

as $j \to \infty$. But $U_j(x, t) - U^*(x, t) = U(jx, jt) - U^*(jx, jt)$ using (5.5) and the fact that U^* must be a similarity solution. So changing variables in (5.7) to $\xi = jx$, $\tau = jt$ gives

$$\frac{1}{j^2} \int_j^{j(1+\delta)} \int_{jm_1}^{jm_2} |U(\xi, \tau) - U^*(\xi, \tau)| \, d\xi \, d\tau \to 0$$

as $j \to \infty$ which is (5.3).

6. Shock tracking and the random choice method. The oscillations observed near shocks with larger ν are presumably caused in large part by interactions between neighboring strong discontinuities that represent a single (smeared) shock. It might be possible to avoid some difficulties by incorporating a simple shock tracking procedure into the algorithm. In addition to a fixed mesh, introduce floating mesh points to represent the strong discontinuities. This avoids smearing of discontinuities. Since there is no Courant number restriction we need not worry about these points falling near the fixed grid points.

Moreover, with this approach we could handle interactions of strong discontinuities (e.g. shock collisions) exactly by shortening the time step when necessary to ensure that approaching shocks land at precisely the same point. Then solving the Riemann problem at the next step would give the correct resolution of the shock collision. This has not been attempted yet but seems promising. A disadvantage is that such an approach is inherently one-dimensional. Another way to maintain sharp discontinuities is to use the random choice method of Glimm [7] (see also Chorin [3] for improvements of the numerical algorithm). This method can also be generalized to larger time steps. In the first description of the large time step algorithm in § 2, we constructed approximate solutions $\tilde{u}^n(x, t)$ which were then averaged at time t_{n+1} to obtain U_i^{n+1}. Alternatively, we could set $U_i^{n+1} = \tilde{u}^n(x_i + \theta_n h, t_{n+1})$ where the θ_n are uniformly distributed random numbers in $[0, 1]$.

An approach that is simpler computationally is the following. As each wave is propagated over the mesh in Algorithm 2.1, the averaging is accomplished in the step

$$U_{i+\mu}^{n+1} := U_{i+\mu}^{n+1} + (\nu - \mu)\Delta u.$$

This can be replaced by

$$U_{i+\mu}^{n+1} := U_{i+\mu}^{n+1} + \delta \Delta u$$

where

$$\delta = \begin{cases} 0 & \text{if } \nu - \mu \leqq \theta_n, \\ 1 & \text{if } \nu - \mu > \theta_n. \end{cases}$$

The effect is that each wave is propagated exactly to a mesh cell boundary. The boundary chosen is the one immediately to the right of the wave's true location with probability $\nu - \mu$ and to the left with probability $1 - \nu + \mu$. Recall that we are assuming the wave velocity is positive and that $\nu - \mu$ is the fraction of the final mesh cell through which the wave propagates. The case when the velocity is negative can be handled similarly.

A hybrid method is also possible in which most waves are averaged and the random choice selection is applied only to strong discontinuities. As an example, this approach has been applied to the problem shown in Fig. 3.6. At time $t = 0.16$ we obtain the results shown in Fig. 6.1. In this simple example the oscillations have been completely eliminated at the expense of some imprecision in the shock location.

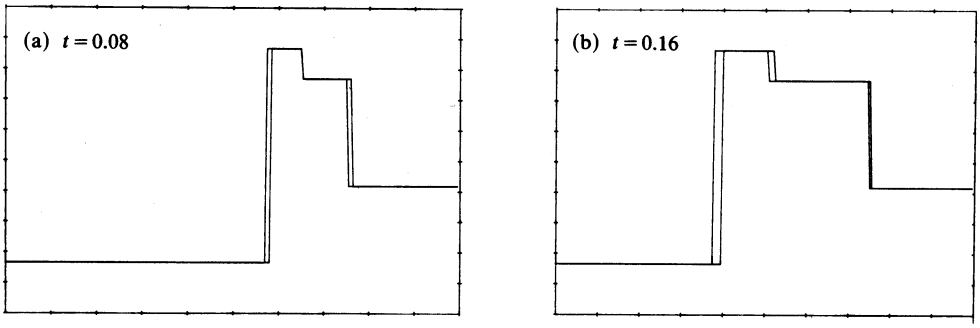

FIG. 6.1. *The density ρ computed using the random choice method with $k = h = 1/400$, superimposed on the true solution. (Courant number ≈ 3.5.)*

7. Conclusions. We have described a method for approximating nonlinear interactions linearly which allows Godunov's method to be applied with arbitrarily large time steps. The numerical results indicate that reasonable results are obtained only with modest values of ν, although the upper bound seems to depend on the degree of nonlinearity of the system and the strength of the shocks present. For smooth solutions good results are obtained even with large ν.

We have only considered generalizing the standard Godunov method but the same linearization could be useful elsewhere as indicated in the introduction. One could also consider other modifications to the method, such as using approximate Riemann solvers in place of the true Riemann solution. For Godunov's method this is now quite standard (cf. [11], [25]). With larger time steps interactions of the resulting approximate waves can again be approximated linearly in a conservative manner [20]. In practice the best approach might be to use the exact Riemann solver on strong discontinuities and the approximate solver on weak discontinuities. This hybrid scheme is still conservative.

Recently a great deal of progress has been made in the construction of stable higher order accurate methods for conservation laws [4], [10], [17], [26], [30]. It is possible that such methods can also be extended to larger time steps. Since the linear approximation of interactions introduces $O(h^2)$ errors in each time step, a direct application of the ideas presented here will not maintain second order accuracy. However, it may be possible, at least for very restricted time steps ($\nu < 2$, say) to modify the corresponding fluxes in a manner akin to that used for $\nu < 1$ [26], [30]. A different approach to constructing higher order large time step methods has been proposed by Harten [9].

In a practical computation it would also be necessary to apply realistic boundary conditions, an issue that has not been discussed here. Some preliminary results indicate that boundaries can be handled reasonably well even with larger time stops. This will be reported on elsewhere.

REFERENCES

[1] Y. BRENIER, *Averaged multivalued solutions for scalar conservation laws*, this Journal, 21 (1984), pp. 1013–1037.

[2] Y. BRENIER, *Averaged multivalued solutions and time discretizations for conservation laws*, to appear in Proc. Fifteenth AMS-SIAM Summer Seminar, AMS Lectures in Applied Mathematics. American Mathematical Society, Providence, RI, 1984.
[3] A. J. CHORIN, *Random choice solution of hyperbolic systems.* J. Comp. Phys., 22 (1976), pp. 517-533.
[4] P. COLELLA AND P. WOODWARD, *The piecewise-parabolic method* (PPM) *for gas dynamical simulations*, J. Comp. Phys., 54 (1984), pp. 174-201.
[5] C. M. DAFERMOS, *Polygonal approximations of solutions of the initial value problem for a conservation law*, J. Math. Anal. Appl., 38 (1972), pp. 33-41.
[6] R. J. DIPERNA, *Convergence of approximate solutions to conservation laws*, Arch. Rat. Mech. Anal., 82 (1983), pp. 27-70.
[7] J. GLIMM, *Solutions in the large for nonlinear hyperbolic systems of equations*, Comm. Pure Appl. Math., 18 (1965), pp. 697-715.
[8] S. K. GODUNOV, *A difference method for numerical calculations of discontinuous solutions of the equations of hydrodynamics*, Mat. Sb., 47 (1959), pp. 271-306. (In Russian.)
[9] A. HARTEN, *On a large time-step high resolution scheme*, ICASE Report No. 82-34, NASA Langley Research Center, Hampton, VA, 1982.
[10] ———, *High resolution schemes for hyperbolic conservation laws*, J. Comp. Phys., 49 (1983), pp. 357-393.
[11] A. HARTEN AND P. D. LAX, *A random choice finite difference scheme for hyperbolic conservation laws*, this Journal, 18 (1981), pp. 289-315.
[12] A. HARTEN, P. D. LAX AND B. VAN LEER, *On upstream differencing and Godunov-type schemes for hyperbolic conservation laws*, SIAM Rev., 25 (1983), pp. 35-62.
[13] A. HARTEN AND J. M. HYMAN, *Self-adjusting grid methods for one-dimensional hyperbolic conservation laws*, J. Comp. Phys., 50 (1983), pp. 235-269.
[14] G. JENNINGS, *Discrete shocks*, Comm. Pure Appl. Math., 27 (1974), pp. 25-37.
[15] P. D. LAX, *Hyperbolic Systems of Conservation Laws and the Mathematical Theory of Shock Waves*, CBMS Regional Conference Series in Applied Mathematics 11, Society for Industrial and Applied Mathematics, Philadelphia, 1973.
[16] P. D. LAX AND B. WENDROFF, *Systems of conservation laws*, Comm. Pure Appl. Math., 13 (1960), pp. 217-237.
[17] B. VAN LEER, *Towards the ultimate conservative difference scheme*, III, J. Comp. Phys., 23 (1977), pp. 263-275.
[18] R. J. LEVEQUE, *Large time-step shock capturing techniques for scalar conservation laws*, this Journal, 18 (1982), pp. 1091-1109.
[19] ———, *Some preliminary results using a large time step generalization of Godunov's method*, Proc. INRIA Workshop on Numerical Methods for the Euler Equations for Compressible Inviscid Flows, INRIA, Rocquencourt, France. Dec. 7-9, 1983, to appear.
[20] ———, *Convergence of a large time step generalization of Godunov's method for conservation laws*, Comm. Pure Appl. Math., 37 (1984), pp. 463-477.
[21] T. P. LIU, *Large-time behavior of solutions of initial and initial-boundary value problems of a general system of hyperbolic conservation laws*, Comm. Math Phys., 55 (1977), pp. 163-177.
[22] D. MARCHESIN AND P. J. PAES-LEME, *Shocks in gas pipelines*, SIAM J. Sci. Stat. Comput., 4 (1983), pp. 105-116.
[23] S. OSHER AND S. R. CHAKRAVARTHY, *High resolution schemes and the entropy condition*, this Journal, 21 (1984), pp. 955-984.
[24] S. OSHER AND J. RALSTON, *L^1 stability of travelling waves with applications to convective porous media flow*, Comm. Pure Appl. Math., 35 (1982), pp. 737-749.
[25] P. L. ROE, *Approximate Riemann solvers, parameter vectors, and difference schemes*, J. Comp. Phys., 43 (1981), pp. 357-372.
[26] ———, *Numerical modelling of shockwaves and other discontinuities*, Proc. IMA Conference on Numerical Methods in Computational Aerodynamics, University of Reading, 1981.
[27] ———, *The use of the Riemann problem in finite difference schemes*, in Proc. Seventh International Conference on Numerical Methods in Fluid Dynamics, W.C. Reynolds and R. W. MacCormack, eds., Lecture Notes in Physics 141, Springer, Berlin 1981.
[28] G. A. SOD, *A survey of several finite difference methods for systems of nonlinear hyperbolic conservation laws*, J. Comp. Phys., 27 (1978), pp. 1-31.
[29] B. K. SWARTZ AND B. B. WENDROFF, AZTEC: *a front tracking code based on Godunov's method*, preprint.
[30] P. K. SWEBY, *High resolution schemes using flux limiters for hyperbolic conservation laws*, this Journal, 21 (1984), pp. 995-1012.